

Fast object detection for use onboard satellites

Martin Bange (bange@faw.uni-ulm.de)*

*Forschungsinstitut für Anwendungsorientierte Wissensverarbeitung Ulm,
Helmholtzstrasse 16, D89081 Ulm, Germany*

Stefan Jordan (jordan@astro.uni-tuebingen.de)

*Institut für Astronomie und Astrophysik, Universität Tübingen, Sand 1, D72076
Tübingen, Germany*

Michael Biermann (mbierman@lsw.uni-heidelberg.de)

Landessternwarte Heidelberg, Königstuhl, D69117 Heidelberg, Germany

Thomas Kämpke (kaempke@faw.uni-ulm.de)

*Forschungsinstitut für Anwendungsorientierte Wissensverarbeitung Ulm,
Helmholtzstrasse 16, D89081 Ulm, Germany*

Ralf-Dieter Scholz (rdscholz@aip.de)

*Astrophysikalisches Institut Potsdam, An der Sternwarte 10, D14482 Potsdam,
Germany*

Abstract. We propose an object detection algorithm which is efficient and fast enough to be used in (almost) real time with the limited computer capacities onboard satellites. For stars below the saturation limit of the CCD detectors it is based on a four neighbourhood local maximum criterion in order to find the centre of a stellar image. For saturated stars it is based on the assumption that the image is increasing monotonically towards the centre in the unsaturated part of the image. The algorithm also calculates approximate stellar magnitudes and efficiently rejects most of the cosemics which would otherwise lead to a large number of false detections. The quality of the algorithm was evaluated with the help of a large set of simulated data for the DIVA satellite mission; different assumptions were made for the noise level, and the presence of cosemics or for a variable sky background. We could show that our algorithm fulfills the requirements for DIVA; only in the case of simulated images which included the bright galaxy M31 some fainter stars could not be detected in the galaxy's vicinity. Since stellar images contain large areas without any stars, we propose an additional block-skipping algorithm which can be coded on special-purpose hardware.

Keywords: CCD image simulation, noise modeling, real-time segmentation.

1. Introduction

Future all-sky space astrometric missions produce huge amounts of data that cannot be sent down to earth. Therefore either only those parts of the sky which are of interest for astronomers (namely small patches around stars or other objects) have to be handpicked for telemetry or all

* corresponding author



astrometrically relevant object parameters have to be computed already on board. The latter will be performed on GAIA, the next ESA astrometric space mission, whereas the former will be chosen for reduction of the downlink rate for DIVA. An object detection algorithm, suitable for DIVA to extract such small patches around detected objects, will be presented in this paper; it is general enough to be adopted to similar mission requirements on other satellites.

DIVA is a small astrometric satellite planned for launch in 2006. It will provide high-precision positions, proper motions, parallaxes and photometric data for some 35 million stars, and spectrophotometric information for about 12 million stars.

A major technical constraint of the DIVA satellite mission is the limited data downlink rate. While 100 Mbit/s of raw data are produced by the DIVA detectors, only 0.7 Mbit/s can be sent to the ground for 17 hours each day. No loss-less compression algorithm is able to account for such a large discrepancy. Moreover, DIVA follows the conservative approach that the astrometric data analysis is completely performed on ground. This, however, means that all data relevant for the astrometric, photometric, and spectroscopic measurements of DIVA have to be selected in real time. For the Sky Mapper CCD detectors (SM1, SM2, see Fig. 1) these are the contents of small rectangular patches of CCD pixels surrounding an object (single or multiple star). Intensive studies with simulated data have shown that sizes of 12×17 are sufficient for stars with DIVA magnitudes $D < 9.5$ and 12×7 for stars down to the limit of $D = 15.2$. DIVA magnitudes are similar to R - and I -magnitudes and have their maximum sensitivity at about 600 nm.

This article mainly deals with the detection and centroiding of stars. Nevertheless, the algorithm presented here also detects non-resolved double stars as well as the dense regions of cores of globular clusters which cannot be resolved by DIVA or any other astrometric space mission but which are well above any reasonable detection limit. In principle, this algorithm can also detect minor planets in the solar system, but this was not tested and is not subject of this paper.

Moreover, it is important to distinguish the objects of interest from detector artifacts, particularly cosmic ray hits (short: cospics) and bad columns. Both tasks – object detection and artifact elimination – have to be performed for SM1 in almost real time on the IPU (Instrument Processing Unit) with only a limited amount of buffer capacity; additionally, the positions of such objects have to be identified on the SM2 detector which were missed due to the gaps between the four SM1 CCD chips.

The scientific data of DIVA do not only consist of the rectangular patches on the SM detectors. Brighter stars ($D < 13.3$) are also seen

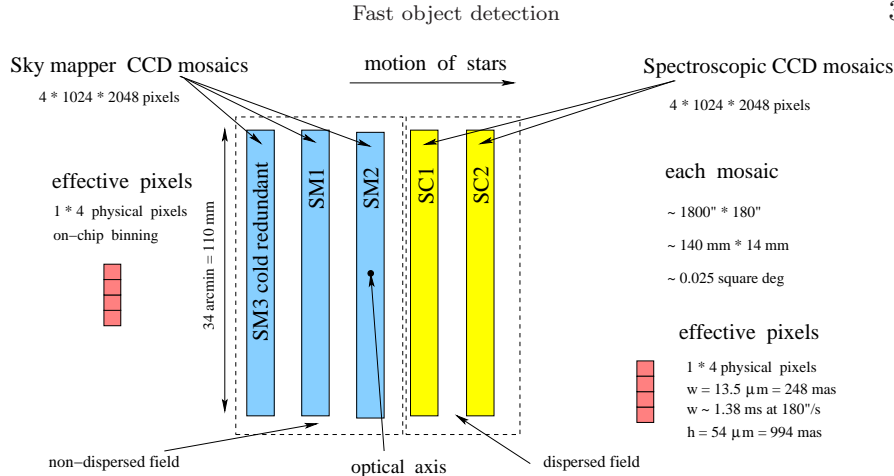


Figure 1. The focal plane layout of DIVA. Object detection will be performed on the four Sky Mapper CCD chips SM1 and in those regions on the slightly shifted SM2 CCDs, which were missed due to gaps between the SM1 chips.

as spectroscopically dispersed images (dispis) on the SC detectors (see Fig. 1). Their positions are predicted from the centres of the objects found by the SM1 (and in a few cases on SM2, respectively). Rectangles containing the dispis are cut out of the SC detectors for further analyses on ground.

DIVA will capture image data in time delayed integration (TDI) mode where the CCD read out is synchronised with the satellite rotation. As a consequence, there are no images in the usual sense of frames but a continuous stream of single lines. For our simulation we will always use 1158 of such lines, corresponding to 1.5 seconds of observations. The resulting frame size $1158 \times 525 \times 4$ (4 CCDs) corresponds to the amount of SM data that can be stored in the IPU ringbuffer.

Section 2 specifies the requirements that must be fulfilled by any appropriate object detection algorithm. Section 3 presents the simulated data, which is the input of the proposed object detection algorithm presented in Section 4. The efficiency and quality of the algorithm is described in Section 5.

2. Requirements

The object detection algorithm should deliver at least 3 output parameters. First of all, the centre of the detected object in pixel coordinates of the corresponding CCD chip characterises the position of the object uniquely. Secondly, the magnitude of each object is needed, in order

to decide if this object must be cut out on the SC chips and to reject stars fainter than a given threshold. Thirdly, cosmic-ray hits have to be distinguished from single stars, double stars and extended objects like the cores of globular clusters.

Around the predicted centre of a detected object some small rectangular patch of pixels is cut out for telemetry. To make sure that all relevant information is included in the pixel array the computed centre of the object must not differ from the real centre of the object by more than 2 effective pixels in each direction.

For on-board software there are additional constraints that do not hold for on-ground software. Firstly, the available RAM for code and data is very limited. It will amount to only 256 or 512 kByte for the DIVA project. Therefore it is not possible to process large parts of data. In fact an effective object detection algorithm should work as local as possible in the sense of a very limited number of CCD lines only. Secondly, the computational power of space-qualified processors is still very low: DIVA will fly with 20 MHz processors so that any code must be designed optimised to meet these requirements.

The quality of an detection algorithm is judged by comparison with the detection probabilities that are prescribed for a particular satellite mission (Bastian and Biermann, 2001). For DIVA they are presented in Table I.

Table I. Required detection probability as a function of the object magnitude

magnitude	detection probability
saturated stars ($D < 8$)	≥ 95 %
$8 \leq D < 14.6$	≥ 99.5 %
$D = 15.2$	(50 ± 5) %

3. Simulation

A sufficiently large amount of simulated SM data including several thousand stars as well as realistic noise, sky and CCD properties is needed in order to investigate the on-board data reduction. The efficiency of the object detection algorithms was tested with 128 simulated frames for the different SM CCD chips. The data have been simulated (Scholz, 2001) based on real sky observations and star catalogues with

a preference given to relatively high stellar density fields, also including some open clusters.

Additionally, 4 of the frames contained the image of the globular cluster M4 (which is relatively sparse). On two frames the dense globular cluster M30 was included in the corner. All stars up to the faintest ones were simulated in case of M30, for which Hubble Space Telescope observations (Guhathakurta et al., 1998) served as input data. On one eighth of all frames a large number of faint (background) objects were present, representing the situation when DIVA scans the Galactic plane; for this purpose we used a catalogue of stars in Baade's window (Szymanski et al., 1996) as input data.

Each CCD chip was modeled with its own characteristic hot and dark columns and a slightly different sensitivity function ($> 90\%$) over the CCD columns (one-dimensional flat field). Conservative noise parameters (dark current of 5 electrons per original pixel and per second, read-out-noise with σ of 7 electrons per effective pixel) and a gain of 3.5 were used, i.e. one signal unit corresponded to 3.5 electrons. A bias level of 30 electrons per effective pixel was added.

The whole data set has also been simulated with optimistic noise parameters (see Fig. 2). The optimistic and conservative CCD noise parameters are defined in the DIVA mission requirements, respectively as optimum and minimum requirements. Optimistic parameters were defined by a dark current of 2 electrons per original pixel and per second and a read-out-noise with a σ of 2 electrons per effective pixel. In case of optimistic noise, a gain of 1 was used, i.e. one signal unit corresponded to 1 electron.

However, the basic simulated data set used in this investigation was that with conservative noise, and it did also include cosmics (see Fig. 3) with a mean number of 70 events per chip field. Cosmics were simply simulated as connected pixels of constant signal (typically 500 electrons). The length of the cosmic ray traces may have been overestimated. The above numbers were estimated for GAIA from experience with the Hubble Space Telescope CCD chips (ESA, 2000).

All simulations included many faint stars far below the envisaged detection limit of $D \sim 15.2$. In total we have considered 19000 stars with 7000 being brighter than $D = 16.1$. Saturated bright stars have also been simulated and added to the data stream with a simplified model on the transfer of charges above the saturation level: Effective pixels with a signal of > 150000 electrons were considered saturated and the charges above the saturation were distributed along the CCD columns in the scan direction (and opposite direction) with a slight asymmetry (more charges transferred in opposite scan direction). A maximum of one saturated star with ($2 \leq D \leq 8$) were randomly added

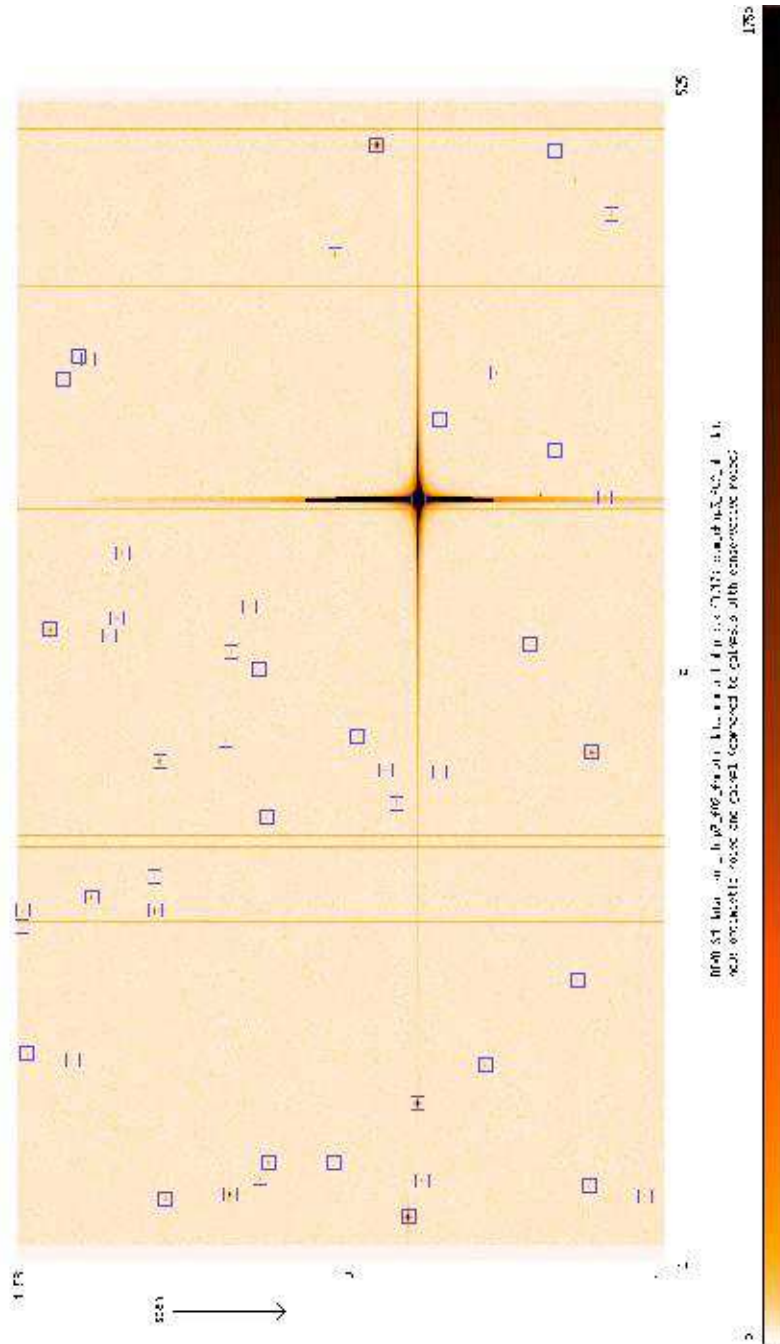


Figure 2. SM chip field of normal stellar density with optimistic noise and without cosmics. Only the brighter simulated objects ($D < 17$) are marked. A very bright saturated star ($D = 2.5$) with its large diffraction spikes has been included in the simulations.

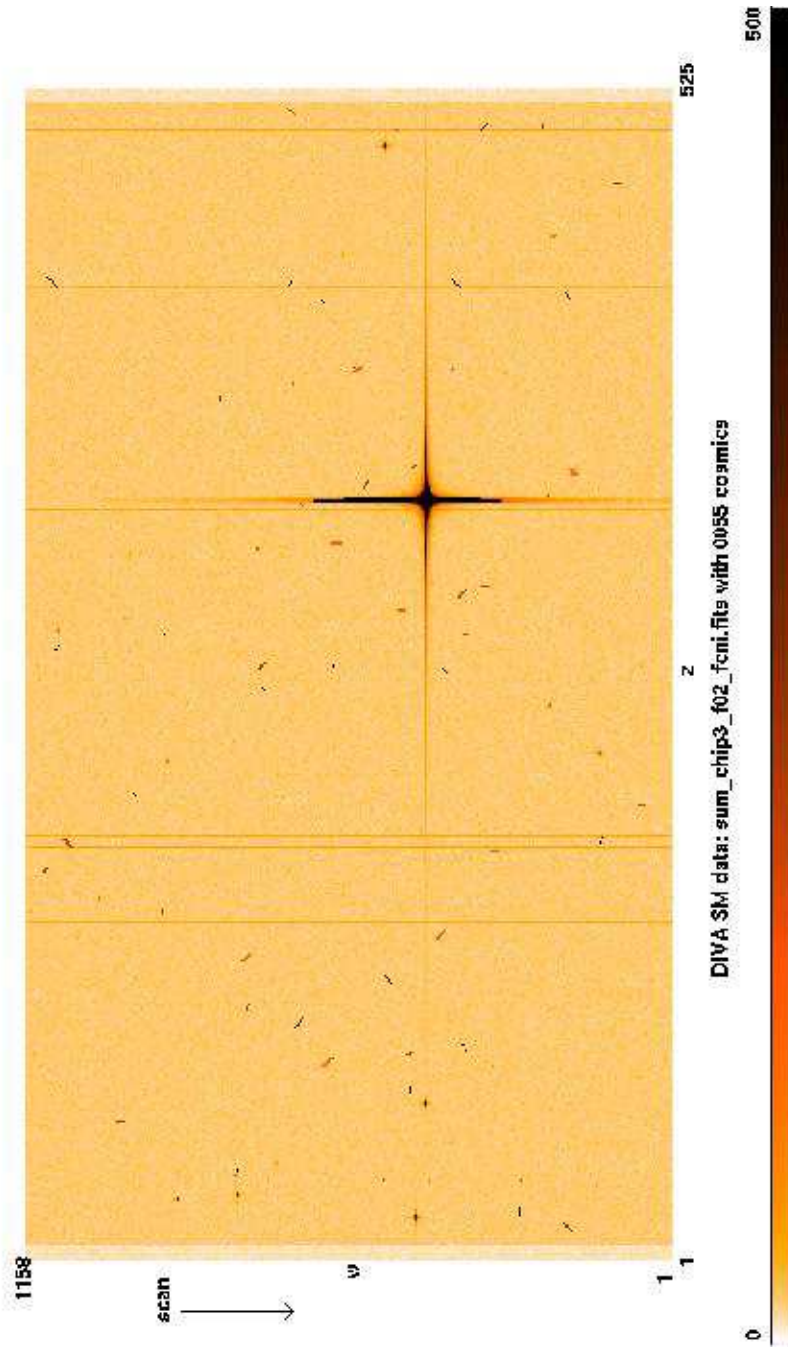


Figure 3. The same SM chip field with conservative noise and with cosmics.

to 27% of the files which is much more frequent than the average during the DIVA mission (about 2%).

In order to be able to test our algorithm for the case of the strongest variation of the background during the DIVA measurements, the M31 galaxy was simulated in the centre of the chip fields and with its major axis in cross-scan direction. The maximum signal in the core of M31 was estimated as 410 electrons per effective pixel. Near to the edge of the chip field (which is about 290×525 arcsec²), the signal from M31 is only about 5 electrons per effective pixel. The conclusion is, that there are no serious background variations to be expected due to extended objects. M31 is certainly one of the brightest extended objects on the sky, but with the short exposure time of 1.5 seconds and the relatively small aperture of DIVA, we see only the core region of M31.

4. Algorithm

In computer vision the detection of stars and their positions with CCD detectors would be called a segmentation problem. In principle, segmentation algorithms for star images may be designed from two extreme perspectives, that of "growing" and that of "shrinking". In the first case an image spot is tentatively or permanently considered to be the centre of a star; then a region is grown or flooded to eventually contain the star. In the other extreme, a candidate region of the image is selected which is likely to contain at least one star. Actual star presence is then tested for the candidate region. In the affirmative case, all star centres must be localised. In both cases, star regions may overlap. Due to conceptual and computational simplicity, the first perspective is adopted here.

In any case, fast segmentation algorithms are typically based on local operations. In astronomy, known examples of such algorithms are SWA (sliding window algorithm) (Babusiaux and Arenou, 1999) and SExtractor (source extractor) (Bertin, 1998). In computer vision in general, object detection under the given time constraints is related to real-time image segmentation for video processing, see for example (Liu et al., 2001). The fundamental difficulty with local segmentation methods is their weak adaptation to global features, such as a slowly varying background level. However, computational studies of adaptive image segmentation algorithms based on entropy (Otsu, 1978) and conditional entropy (Johannsen and Bille, 1982) revealed unacceptably high computation times for the present problem. To what extent a varying background may be a problem is considered by testing our algorithm on frames containing the bright galaxy M31.

We propose a simple detection and centroiding algorithm for DIVA which is motivated by the fact that a local maximum in a stellar image is very close to the position (centre) of the star. However, for stars above the saturation threshold of the CCD detector a different treatment is necessary.

The proposed algorithm identifies pixels that are local intensity maxima and that exceed a certain threshold. These pixels become candidates for star centres. Each candidate undergoes several tests and is accepted as star centre if and only if it passes all of them. All tests are local (and therefore fast) considering at most a 3×3 window around the centre candidate pixel.

More precisely, a pixel p is selected as the centre of a stellar candidate if the pixel intensity $I(p)$ exceeds the detection threshold

$$T = B + 4 \cdot \sqrt{B}, \quad (1)$$

where B is the background. Here the assumption was made that the noise is poissonian. This is no serious limitation because the factor of 4 can be easily changed to a different value; slight adaptations are always possible during the commissioning phase of DIVA or whenever necessary. For the background value B we used the median of the simulated images since it is a very robust estimate in almost all astronomical images. For the on-board IPU software of DIVA we plan to use an approximate median from 81 points for several sampling regions on the SM detectors. The value is calculated by a special purpose hardware in a 4 stage pipeline, which in each step calculates the median of triples only (see (DIVA, 2002)). In this paper we assume a constant background over one simulated frame. For DIVA, however, we plan smaller sampling regions to better account for varying background.

Since CCD detectors have a limited dynamic range, a special treatment is necessary for saturated stellar images. Therefore, we have to distinguish between star candidates above saturation threshold T_S and those below this limit but exceeding the detection threshold.

The pseudo code of this procedure is as follows.

```

/* Main part */
T = bg + 4 * squareroot(bg); /* bg = median of the image */
FOR (every image row) DO
  FOR (every pixel in the current row) DO
    IF (intensity > T) AND (intensity ≤ TS) THEN
      analyse_unsaturated_object();
    ELSEIF (intensity > TS) THEN
      analyse_saturated_object();
    ENDIF
  
```

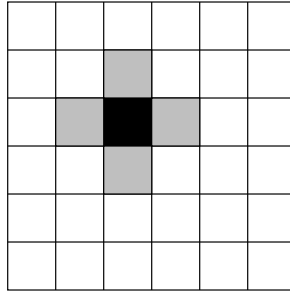


Figure 4. The currently considered pixel (black) with its neighbourhood of four pixels which are tested for having a smaller value.

```

ENDFOR
  IF (analysis of a saturated object is completed) THEN
    save object coordinates;
  ENDIF
ENDFOR

```

4.1. UNSATURATED STARS

The analysis for an unsaturated star is based on the intensity $I(p)$ of the current pixel p exceeding the detection threshold T and staying below the saturation limit T_S . In order to be the centre of a star the pixel p has to pass some additional tests.

One feature of an unsaturated star is that its centre represents a local intensity maximum. Therefore $I(p)$ has to exceed the value of each of its neighbouring pixels (neighbourhood of four, see Fig. 4) or at least the value of three neighbouring pixels and to be equal to the fourth one. The latter case can be caused by noise. It is possible that even more than two pixels in the centre area of an unsaturated star have the same value. But in practice this is unlikely.

In order to be regarded as a star, N of the four neighbours have to exceed the detection threshold. N was determined experimentally and depends on the data set. For conservative noise $N = 2$ was chosen and for optimistic noise $N = 3$ was chosen. The value had to be lowered for conservative noise because otherwise too many stars in the magnitude range $8.0 \leq D < 14.6$ would have been lost. This condition helps to eliminate some cosmics, noise peaks and detections on hot columns.

If the current pixel passed the foregoing tests, measures for the star magnitude and a measure for the likelihood to be a cosmic are computed. In order to determine the magnitude, the 3×3 window W surrounding the current pixel is used. Only those pixels p_i in this

window with an intensity $I(p_i) > T$ are taken into account for the magnitude computation which is as follows:

$$m = \sum_{\{p_i \in W | I(p_i) > T\}} (I(p_i) - B) \quad (2)$$

This value must exceed a magnitude threshold T_m . Otherwise the current pixel cannot belong to a sufficiently bright star. T_m depends on the data set and will be calibrated during the commissioning phase. Simulations have shown that the accuracy of the magnitude determination (1σ) is $\Delta D \approx 0.15$ at $D < 15$ and 0.5 at $D \geq 15$. For saturated stars no magnitude determination was performed. A serious problem arises from cosmics. As described in Section 3 we can expect about 70 cosmics per image. Many of them will pass the three previous tests. Moreover, the algorithm often detects more than one local maximum per cosmic (in the average), increasing the rate of false detections extremely. Hence it is crucial that the algorithm is able to filter out most of such false detections. In contrast to a star, the intensity values of a cosmic form a plateau with arbitrary orientation. This is different from the appearance of a star where we have a sharp maximum which is significantly higher than the average intensity of the other pixels belonging to the star image. Thus, for cosmic rejection, the difference

$$I(p) - \frac{m}{n} \quad (3)$$

can be used as indicator, where $n = |\{p_i \in W | I(p_i) > T\}|$. This difference is sufficient to distinguish between cosmics and bright stars. However, for fainter stars close to the DIVA limit of about $D = 15.2$ we had to take the dependence of this difference from the magnitude of a star into account. Therefore, the above difference is set in relation to the average magnitude per pixel. Cosmics have a higher average magnitude compared to faint stars. The fraction

$$c = \frac{I(p) - m/n}{m/n} \quad (4)$$

is used to distinguish stars from cosmics and is a measure for the likelihood to be a cosmic. In order to treat an object as a cosmic, c must exceed a threshold T_c which depends on the data set and which has to be calibrated during the commissioning phase. This criterion also helps to sort out some false detections on hot columns. The pseudo code of this analysis is as follows:

```
/* analyse_unsaturated_object() */
IF (current pixel is a local maximum) AND
```

```

(N of the 4 neighbours exceed T) THEN
  IF (magnitude >  $T_m$ ) AND ( $c > T_c$ ) THEN
    save object coordinates and magnitude value;
  ENDIF
ENDIF

```

4.2. SATURATED STARS

A saturated star image, which contains at least one pixel above the saturation threshold $T_S \gg T$, can differ drastically from that of unsaturated stars so that a special treatment is necessary. In this case a mere local maximum search over intensities does not find the centres of saturated stars within the required precision. For this reason, the detection algorithm for saturated stars allows for a mixed mode of maximum search. This mixed mode considers intensity values as well as sets of adjacent pixels above saturation threshold.

The treatment of saturated star images depends on the point spread function in the focal plane. Our algorithm is based on the assumption that the point spread function is monotonically increasing towards the centre of the star, which is the case of the cross-like star image caused by the rectangular apertures of the DIVA telescopes.

Let (i, j) be a pixel above saturation level. Let this pixel be the first saturated pixel in the scanning sequence which means that its left neighbour (in same row i) and its upper neighbour (in same column j) are unsaturated.

Scanning the preceding row $i - 1$ leads to the column coordinate of the centre of the saturated star. Starting from pixel $(i - 1, j)$, row $i - 1$ is scanned to the left as long as intensities increase in this direction. Then the maximum search is continued from pixel $(i - 1, j)$ in the right direction, again as long as intensities increase. The column index of the resulting maximum corresponds to the column index of the centre.

The row index of the centre is found as follows: Beginning with pixel (i, j) , a set of consecutive pixels in row i is scanned to the right until intensities drop below the saturation threshold. This is repeated for saturated pixels $(i + 1, j)$, $(i + 2, j)$ etc. as long as the number of these adjacent pixels above saturation threshold increases from row to row. The scanning extends to both the left and the right direction for rows $i + 1$, $i + 2$ etc. The row of the largest of such intervals is selected as the row index of the star centre. This contains a monotonicity criterion: The number of connected saturated pixels increases from row to row as long as the centre of the star is not reached.

Fig. 5 shows the saturated pixels of a star and illustrates the algorithm. Technically, the search for the row index is done only towards the

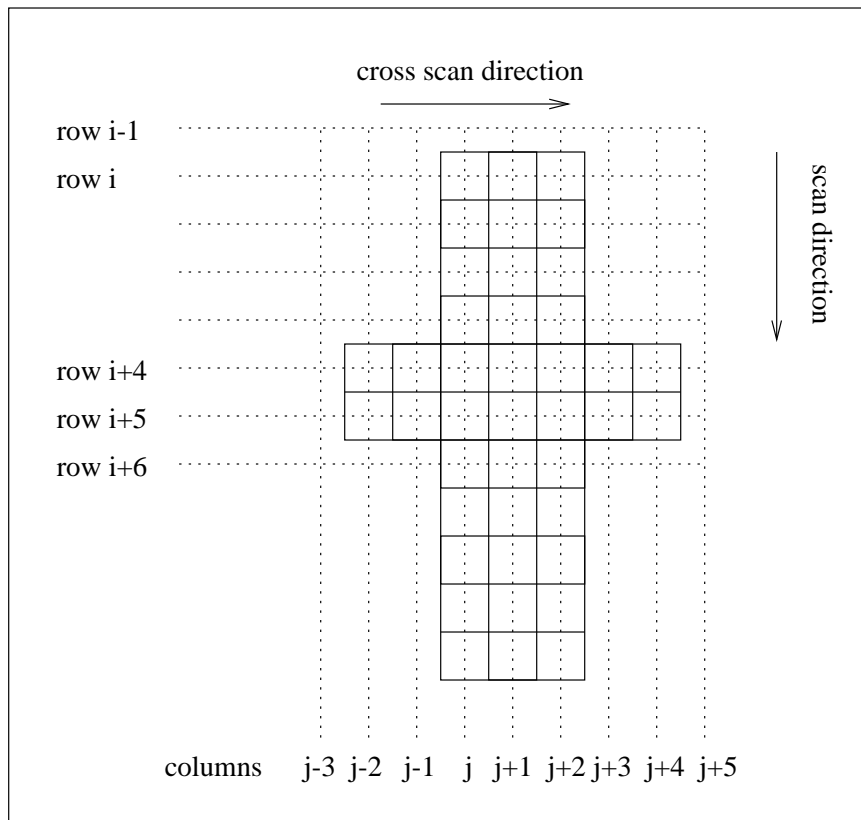


Figure 5. Illustration of the algorithm for saturated stars.

right. It may then happen, that one saturated star is scanned starting from different saturated pixels. Different candidate regions of saturated stars are treated as one single object if they have one saturated pixel in common.

```

/* analyse_saturated_object() */
determine number S of connected saturated pixels of the
  star in the current row;
IF (current row is the first row that contains saturated
  pixels of the current object) THEN
  search the pixels in the previous row that belong to the
  current object for their maximum;
  cross scan coordinate of centre = cross scan coordinate
  of the found maximum;
/* Initialise scan coordinate of the centre */
scan coordinate of centre = index of the current row;

```

```

maximum in scan direction = intensity of the first
  unsaturated pixel to the left or to the right of the
  saturated pixels;
ELSE
  IF (S(current row) > S(previous row)) THEN
    scan coordinate of centre = index of current row;
    maximum in scan direction = intensity of the first
      unsaturated pixel to the left or to the right of
      the saturated pixels;
  ELSEIF S(current row) == S(previous row) THEN
    IF (maximum in scan direction) <= (intensity of
      the first unsaturated pixel to the left or to the
      right of the saturated pixels) THEN
      scan coordinate of centre = index of current row;
      maximum in scan direction = intensity of the first
        unsaturated pixel to the left or to the right of
        the saturated pixels;
    ENDIF
  ENDIF
ENDIF
ENDIF
ENDIF

```

4.3. ACCELERATION BY BLOCK SKIPPING

The star detection algorithm as developed so far compares every pixel value with the detection threshold. But large parts of the sky are empty in the sense that there are no interesting objects, i.e. no pixels with intensities above the threshold. If the algorithm can skip these parts, computation time will be saved.

Therefore, the first k pixel values of a row are compared to the detection threshold T . If one of these intensities exceeds the threshold, a header bit for this block is set to one. Otherwise the header bit is set to zero. Then the next k pixel values of this row are compared to T . Accordingly to the result a second header bit is set. This is continued until the end of the row. This procedure is executed for each row. The star detection algorithm will be run only for those blocks whose header bits equal one. It is run for all pixels of such blocks. Such a simple identification of interesting blocks can be easily done with special purpose hardware chips and would therefore relieve the on-board computer significantly.

5. Evaluation

The algorithm was tested with all four sets of simulated data (conservative and optimistic noise, each for the case with and without cosmics). The results for the different data sets are shown in the Table II. The first column in our tables of results describes the real (prescribed) magnitude of the star, not the computed one. In the following columns the detection rates for all data sets are given. A star is regarded as detected correctly if the centre determined by the algorithm agrees with the simulated image location within two pixels in both coordinates and if the detected star is brighter than $D = 16.1$. On the other side a false detection occurs if no simulated star image brighter than $D = 16.1$ lies within two pixels of the detection's location indicator in both coordinates.

Table II. Detection rates for the data sets with conservative noise and optimistic noise, each including and without cosmics. The corrected false detection rate takes into account that the number of false detections which are due to bright stars is lower in reality by a factor of 14.

Magnitude	det. rate w.o. cosmics conservative noise	with cosmics conservative noise
$D < 8.0$ (saturated)	100%	100%
$8.0 \leq D < 14.6$	99.6%	99.5%
$D \approx 15.2$	47.1%	47.5%
False detections	16.8%	21.3%
False detections (corr.)	2.1%	6.0%
Magnitude	det. rate w.o. cosmics optimistic noise	with cosmics optimistic noise
$D < 8.0$ (saturated)	100%	100%
$8.0 \leq D < 14.6$	99.7%	99.6%
$D \approx 15.2$	51.5%	49.0%
False detections	12.9%	16.2%
False detections (corr.)	1.8%	6.2%

It turned out that the algorithm is successful in centroiding saturated stars. For $8.0 \leq D < 14.6$ it also fulfills the requirement of 99.5%, specified for the DIVA satellite mission. Two of the simulated stars in this magnitude range (corresponding to about 0.1%) could not be detected because they were too close to a much brighter star.

Therefore, the centres of the two fainter stars do not represent local maxima in this environment.

The cosmic criterion allows us to achieve the required detection rates for $D \approx 15.2$ while keeping the false detections in an acceptable range. Most of these false detections are caused by local maxima that arise on the axes of saturated stars because of noise. This problem could be further mitigated with the aid of the cosmic criterion but only at the expense of the positive detections ($8.0 < D \leq 14.6$ and $D \approx 15.2$). A minor part of the false detections is caused by hot columns; they were reduced considerably by a division of the bad columns by a factor of 2. This factor has to be optimized during the commissioning phase. In reality the number of false detections would be much smaller, since the majority of them are due to the presence of bright saturated stars. Since our simulations have included a factor of 14 more bright objects than in an average region of the sky, we have listed a corrected value in the table for which we have divided the number of false detections which were due to bright stars by this factor.

5.1. RESULTS FOR M31

In order to test whether a variable background would affect the detection rate of our algorithm we additionally applied it to the simulated data sets containing the galaxy M31 (see section 3). M31 can be considered as a worst case since it has a very large surface brightness in its core. For these data sets we obtained the following results:

Table III. Detection rates for the data set containing M31 assuming conservative noise and the presence of cosmics. Since most of the false detections were due to the bright core of M31 a corrected false detection rate was not listed.

Magnitude	detection rate
$D < 8.0$ (saturated)	100%
$8.0 \leq D < 14.6$	99.6%
$D \approx 15.2$	39.7%
False detections	511.8%

The presence of M31 has almost no influence on the rate of successful detection. The only problem is caused by false detections in the very neighbourhood of the galaxie's core. This is very similar to some false detections caused by noise peaks close to bright saturated stars. M31's

core creates an area on the CCD which is above the detection threshold so that this single criterion is always fulfilled. If then, due to noise, a pixel is a local maximum, it is treated as a star. However, even the high number of false detections would cause no real limitations, because they are restricted to extremely small areas of the sky. Although the described algorithm has not been tested on the DIVA computer hardware, we believe that this peak can still be handled (from conservative estimations we expect that we can handle about 300-1000 detections per second). Since M31 can be regarded as a worst case, we do not expect similar problems elsewhere. If we were, due a data overflow, forced to disregard a part of the stars in this region, this would only lead to a smaller number of measurements since not always the same stars would be lost.

6. Conclusion

Our very simple four-neighbourhood local maximum method together with some special algorithms for saturated stars, cosmic detection, and magnitude determination turned out to fulfill the requirements of astrometric satellite missions like DIVA: It is fast, finds the centres of nearly all stars down to $D = 14.6$ and most at the limit of $D = 15.2$, rejects cosmics very efficiently, calculates the stellar magnitudes with sufficient precision, and has a very low number of false detections. The number of wrong identifications only increases in the neighbourhood of bright extended objects like extremely bright and saturated stars or the cores of bright galaxies. Since such peaks correspond to only very small areas of the sky (corresponding to only fractions of a second during DIVA measurements) they do not pose major difficulties.

A comparison of our method with other local segmentation algorithms has shown it's superiority in both speed and reliability. As an example we have tested the efficiency of the local SExtractor and SWA algorithms and found that their ability to detect bright and saturated stars was well below the requirements. Alternatives to local detection like adaptive image segmentation algorithms based on entropy and conditional entropy would cause a need for more memory for the on-board computer than usually available on space missions.

Acknowledgements

Algorithm development was supported in part by Astrium company under DLR grant 50 QD 0106/F 39260. Stefan Jordan and Michael

Biermann were supported by DLR grants 50 QD 0109 and 50 QD 0101, respectively.

References

- Babusiaux, C., Arenou, F., "A possible detection algorithm for GAIA", 1999.
- Bastian, U., Biermann, M., "DIVA: Criteria for successful on-board image detection", 2001, DIVA archive TD0265-03
- Bertin, E., "SExtractor user's guide", 1998, www.eso.org/science/eis/eis_doc/sex2/sex2html/sex2_doc.html.
- Bratsolis, E., Sigelle, M., "Solar image segmentation by use of mean field fast annealing", *Astronomy & Astrophysics Supplement Series* 131, 1998, p. 371-375.
- DIVA, Preliminary Design Review documentation, 2002.
- ESA 2000, "GAIA: Composition, Formation and Evolution of the Galaxy, Concept and Technology Study Report", ESA-SCI(2000)4, July 2000, 381 pp.
- Guhathakurta P., Webster Z.T., Yanny B., Schneider D.P., Bahcall J.N., "Globular cluster photometry with the Hubble Space Telescope. VII. Color gradients and blue stragglers in the central region of M30 from Wide Field Planetary Camera 2 observations", 1998, *AJ*, 116, 1757.
- Johannsen, G., Bille, J., "A threshold selection method using information measures", *Proceedings 6th International Conference on Pattern Recognition ICPR*, Berlin, 1982, p. 140-143.
- Liu, T., Kender, J.R., Hjelsvold, R., Pizano, A., "A fast image segmentation algorithm for interactive video hotspot retrieval", *IEEE Workshop on Content-Based Access of Image and Video Libraries*, 2001, www.cs.columbia.edu/~tliu/download/cbaivl_2001.pdf.
- Otsu N., "A threshold selection method from gray-scale histograms", *IEEE Transactions on Systems, Man, and Cybernetics* 8, 1978, p. 62-66.
- Scholz R.-D., "Simulated DIVA Skymapper (SM) data for test of on-board detection", 2001, DIVA-DF0003-01 and DIVA-DF0004-01 (DIVA data archive - <http://www.ari.uni-heidelberg.de/diva/diva.archive>).
- Szymanski M., Udalski A., Kubiak M., Kaluzny J., Mateo M., Krzeminski W., "The Optical Gravitational Lensing Experiment. The General Catalog of Stars in the Galactic Bulge. I. The Stars in the Central Baade's Window OGLE Field BWC", 1996, *Acta Astronomica*, v.46, pp.1-8.